

## An analytical solution for finitely long hollow cylinder subjected to torsional impact

X. Wang<sup>†</sup>, X. Y. Wang<sup>‡</sup> and W. H. Hao<sup>‡†</sup>

*Department of Engineering Mechanics, The School of Civil Engineering and Mechanics,  
Shanghai Jiaotong University, Shanghai 200240, P. R. China*

*(Received August 11, 2003, Accepted October 21, 2004)*

**Abstract.** An analytical method is presented to solve the elastodynamic problem of finitely long hollow cylinder subjected to torsional impact often occurs in engineering mechanics. The analytical solution is composed of a solution of quasi-static equation satisfied with the non-homogeneous boundary condition and a solution of dynamic equation satisfied with homogeneous boundary condition. The quasi-static solution is obtained directly by solving the quasi-static equation satisfied with the non-homogeneous boundary condition. The solution of the non-homogeneous dynamic equation is obtained by means of finite Hankel transform on the radial variable,  $r$ , Laplace transform on time variable,  $t$ , and finite Fourier transform on axial variable,  $z$ . Thus, the solution for finitely long, hollow cylinder subjected to torsion impact is obtained. In the calculating examples, the response histories and distributions of shear stress in the finitely long hollow cylinder subjected to an exponential decay torsion load are obtained, and the results have been analyzed and discussed. Finally, a dynamic finite element for the same problem is carried out by using ABAQUS finite element analysis. Comparing the analytical solution with the finite element solution, it can be found that two kinds of results obtained by means of two different methods agree well. Therefore, it is further concluded that the analytical method and computing process presented in the paper are effective and accurate.

**Key words:** torsional impact; finitely long hollow cylinder; elastodynamic; integral transform.

---

### 1. Introduction

In many applied engineering fields, a notable problem is the determination of dynamic shear stress in a structure subjected to torsional impact load. This dynamic stress may affect the dynamic strength of the structure. Torsional impact can take place in many different engineering applications such as machine drilling, geologic exploration drilling, structural bolt fastening. Previous researches on theoretical solutions for structures under impact loads have mainly focused on radial impact (Cho *et al.* 1998, Eringen and Suhubi 1975, Pao and Ceranoglu 1978, Cinelli 1965, 1966, Soldatos and Ye 1994, Wang *et al.* 2000). General solution methods used for thick-walled cylindrical shell dynamic problems are: the integral transform method (Cho 1998), the eigen-function method (Eringen and Suhubi 1975), the ray method (Pao and Ceranoglu 1978) and the finite Hankel

---

<sup>†</sup> Professor, Corresponding author, E-mail: [xwang@mail.sjtu.edu.cn](mailto:xwang@mail.sjtu.edu.cn)

<sup>‡</sup> Doctor

<sup>‡†</sup> Master

transform (Cinelli 1965). The theoretical solution of thick-walled shells under torsional impact has seldom been considered so far. Liu and Wang (1995) give the response histories of semi-infinite and infinite elasto-body under a torsional force with time and uniform distribution along the length of cylinders. Kim and Haim (1991) presented the response histories of shear stress wave in a cylindrical wave-guide tube with longitudinal section periodic changing by using the theory of elasticity and experiments. Clark (1956) investigated torsional wave propagation in hollow cylindrical bars. Gazis (1995a, 1995b) presented three-dimensional investigation of the propagation of waves in hollow circular cylinders. Armenákas (1965) researched torsional waves in composite rods. An approximate theory of torsional wave propagation in elastic circular composite cylinders was presented by Haines and Lee (1971). Carcione and Seriani (1998) has given the propagation of torsional waves in lossy cylinders. A simulation of stress waves in attenuating trill strings, including piezoelectric sources and sensors was presented by Carcione and Flavio (2000). Cinelli (1966) gives a theoretical solution for a hollow cylinder under torsional impact by making use of the finite Hankel transform. After analysis, the theoretical solution given in Cinelli (1966) was seen to be manifestly incorrect and no examples were given. Due to the complexity of the problem, the investigations on the propagation of torsional wave in a finitely long hollow cylinder are only a few.

This paper develops analytical equations for elastodynamic problem of finitely long hollow cylinder, with mixed boundary conditions under torsional impact loading. The analytic expressions of the tangent displacement and the shear stress in the finitely long cylinder subjected to torsional impact load are obtained by means of a finite Hankel transform on the radial variable  $r$ , Fourier transform on axial variable  $z$  and Laplace transform on time variable  $t$ .

In the example calculations, the histories and the distributions of shear stress in the finitely long hollow cylinder subjected to torsional impact load are presented. By analyzing the calculated results, it is found that the solution has the wave's properties, and appears in a strong discontinuity effect at the shear stress wavefront. Finally, a dynamic finite element is carried out for the same problem by using ABAQUS finite element analysis. Comparing the analytical solution with the finite element solution, it is manifested that the method and the calculating procedure presented in the paper is concise and practicable, has certain practical applications to similar questions.

## 2. Dynamic equation and solution for torsional problem

A finitely long hollow cylinder with the outer boundary fastened and inner wall subjected to a torsional impact load  $A(z, t)$  is shown in Fig. 1. Considering the geometry and loading shown in Fig. 1, this is seen to be an axisymmetric problem. Therefore, in the cylindrical coordinate system, all the strain variables are independent of  $\theta$ , and  $U_r = U_z = 0$ . Thus, geometrical equations, stress-strain relations and equilibrium equations can be, respectively, expressed as

$$\gamma_{\theta z} = \frac{\partial U_{\theta}(r, z, t)}{\partial z}, \quad \gamma_{r\theta} = \frac{\partial U_{\theta}(r, z, t)}{\partial r} - \frac{U_{\theta}(r, z, t)}{r} \quad (1)$$

$$\tau_{\theta z} = G \frac{\partial U_{\theta}(r, z, t)}{\partial z}, \quad \tau_{r\theta} = G \left( \frac{\partial U_{\theta}(r, z, t)}{\partial r} - \frac{U_{\theta}(r, z, t)}{r} \right) \quad (2)$$

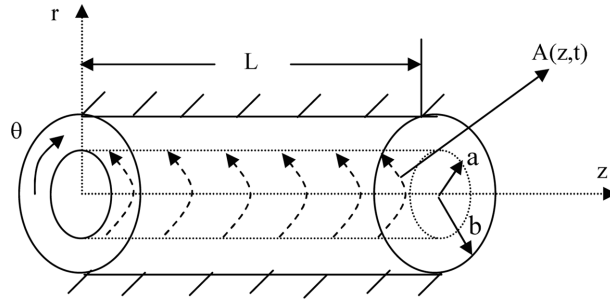


Fig. 1 The structural model

$$\frac{\partial \tau_{r\theta}(r, z, t)}{\partial r} + \frac{\partial \tau_{\theta z}(r, z, t)}{\partial z} + \frac{2\tau_{r\theta}(r, z, t)}{r} = \rho \frac{\partial^2 U_\theta(r, z, t)}{\partial t^2} \quad (3)$$

where  $U_\theta(r, z, t)$  expresses tangential displacement,  $G$  expresses shear module and  $\rho$  expresses the density of material.

From Eqs. (2) and (3), the elastodynamic equation is written as

$$\frac{\partial^2 U_\theta(r, z, t)}{\partial r^2} + \frac{1}{r} \frac{\partial U_\theta(r, z, t)}{\partial r} - \frac{U_\theta(r, z, t)}{r^2} + \frac{\partial^2 U_\theta(r, z, t)}{\partial z^2} = \frac{1}{C_\tau^2} \frac{\partial^2 U_\theta(r, z, t)}{\partial t^2} \quad t \geq 0 \quad (4)$$

where  $C_\tau = \sqrt{G/\rho}$  is the velocity of shear stress wave.

Boundary condition:

$$\begin{aligned} r = a, \quad \tau_{r\theta}(r, z, t) &= G \left( \frac{\partial U_\theta(r, z, t)}{\partial r} - \frac{U_\theta(r, z, t)}{r} \right) = A(z, t) \\ r = b, \quad U_\theta(r, z, t) &= 0 \end{aligned} \quad (5)$$

Ends condition:

$$\begin{aligned} z = 0, \quad \tau_{\theta z}(r, z, t) &= G \frac{\partial U_\theta(r, z, t)}{\partial r} = 0 \\ z = l, \quad \tau_{\theta z}(r, z, t) &= G \frac{\partial U_\theta(r, z, t)}{\partial r} = 0 \end{aligned} \quad (6)$$

Initial condition:

$$t = 0, \quad U_\theta(r, z, t) = U_{\theta 0}(r, z), \quad \frac{\partial U_\theta(r, z, t)}{\partial t} = V_{\theta 0}(r, z) \quad (7)$$

The solution of Eq. (4) can be expressed as

$$U_\theta(r, z, t) = U_{\theta s}(r, z, t) + U_{\theta d}(r, z, t) \quad (8)$$

where  $U_{\theta s}(r, z, t)$  is defined as a quasi-static solution which satisfies a homogeneous quasi-static equation with inhomogeneous boundary condition and  $U_{\theta d}(r, z, t)$  is a dynamic solution which satisfies an inhomogeneous dynamic equation with homogeneous boundary conditions.

The quasi-static equation is expressed as

$$\frac{\partial^2 U_{\theta_s}(r, z, t)}{\partial r^2} + \frac{1}{r} \frac{\partial U_{\theta_s}(r, z, t)}{\partial r} - \frac{U_{\theta_s}(r, z, t)}{r^2} = 0 \quad (9)$$

The corresponding inhomogeneous boundary condition is

$$\begin{aligned} r = a, \quad G \left( \frac{\partial U_{\theta_s}(r, z, t)}{\partial r} - \frac{U_{\theta_s}(r, z, t)}{r} \right) &= A(z, t) \\ r = b, \quad U_{\theta_s}(r, z, t) &= 0 \end{aligned} \quad (10)$$

Solving Eq. (9) and applying inhomogeneous boundary condition (10), we have

$$U_{\theta_s}(r, z, t) = \frac{a^2}{2G} \left( \frac{r}{b^2} - \frac{1}{r} \right) A(z, t) \quad (11)$$

From Eqs. (4), (8), (9) and (10), the inhomogeneous dynamic equation with the corresponding boundary and initial condition are, respectively, represented as

$$\begin{aligned} \frac{\partial^2 U_{\theta_d}(r, z, t)}{\partial r^2} + \frac{1}{r} \frac{\partial U_{\theta_d}(r, z, t)}{\partial r} - \frac{U_{\theta_d}(r, z, t)}{r^2} &= \frac{1}{C_\tau^2} \left( \frac{\partial^2 U_{\theta_s}(r, z, t)}{\partial t^2} + \frac{\partial^2 U_{\theta_d}(r, z, t)}{\partial t^2} \right) - \\ &\left( \frac{\partial^2 U_{\theta_s}(r, z, t)}{\partial z^2} + \frac{\partial^2 U_{\theta_d}(r, z, t)}{\partial z^2} \right) \end{aligned} \quad (12)$$

$$\left[ \frac{\partial U_{\theta_d}(r, z, t)}{\partial r} - \frac{U_{\theta_d}(r, z, t)}{r} \right]_{r=a} = 0, \quad [U_{\theta_d}(r, z, t)]_{r=b} = 0 \quad (13)$$

$$U_{\theta_d}(r, z, 0) = U_{\theta_0}(r, z) - U_{\theta_{s0}}(r, z), \quad \frac{\partial U_{\theta_d}(r, z, 0)}{\partial t} = V_{\theta_0}(r, z) - V_{\theta_{s0}}(r, z) \quad (14)$$

In Eq. (12), the  $U_{\theta_s}(r, z, t)$  is the known quasi-static solution shown in Eq. (11).

The homogeneous form of Eq. (12) can be written as

$$\frac{\partial^2 U_d(r, z)}{\partial r^2} + \frac{1}{r} \frac{\partial U_d(r, z)}{\partial r} + \left( \xi^2 - \frac{1}{r^2} \right) U_d(r, z) = 0 \quad (15)$$

The general solution for Eq. (15) is written as

$$U_d(r, z) = B_1(z)J_1(\xi r) + B_2(z)Y_1(\xi r) \quad (16)$$

where  $J_1(\xi r)$  and  $Y_1(\xi r)$  are, respectively, first order Bessel function of the first and the second kinds,  $B_1(z)$  and  $B_2(z)$  are arbitrary function. From Eq. (16) and Eq. (13), we have

$$\begin{aligned} B_1(z) \left[ \xi J_1'(\xi a) - \frac{1}{a} J_1(\xi a) \right] + B_2(z) \left[ \xi Y_1'(\xi a) - \frac{1}{a} Y_1(\xi a) \right] &= 0 \\ B_1(z)J_1(\xi b) + B_2(z)Y_1(\xi b) &= 0 \end{aligned} \quad (17a,b)$$

Substituting Eq. (17b) into Eq. (16) yields

$$U_d(r, z) = \frac{B_1(z)}{Y_1(\xi b)} [J_1(\xi r)Y_1(\xi b) - J_1(\xi b)Y_1(\xi r)] \tag{18}$$

From Eq. (17), an eigenequation is given by

$$Y_1(\xi_i b)J_a - J_1(\xi_i b)Y_a = 0 \tag{19}$$

where  $J_a = \xi J'_1(\xi a) - \frac{1}{a}J_1(\xi a), \quad Y_a = \xi Y'_1(\xi a) - \frac{1}{a}Y_1(\xi a)$  (20)

$\xi_i (i = 1, 2, 3, \dots)$  are the positive real eigenroots of the eigen Eq. (19).

Eq. (16) can be rewritten as

$$U_{di}(r, z) = B_i(z)C_1(\xi_i r) \tag{21}$$

where,  $B_i(z) = B_{1i}(z)/Y_1(\xi_i b), \quad C_1(\xi_i r) = J_1(\xi_i r)Y_1(\xi_i b) - J_1(\xi_i b)Y_1(\xi_i r)$  (22)

Applying the normalization of  $C_1(\xi_i r)$ , from Eq. (21) we have

$$B_i(z) = \frac{\int_a^b U_{di}(r, z)C_1(\xi_i r)rdr}{\int_a^b C_1^2(\xi_i r)rdr} \tag{23}$$

Apparently, from a serial of  $U_{di}(r, z)(i = 1, 2, 3, \dots)$ , the general expression of  $U_d(r, z)$  can be represented as

$$U_d(r, z) = \sum_{\xi_i} B_i(z)C_1(\xi_i r) \tag{24}$$

Let finite Hankel transform of  $U_d(r, z)$  be defined as

$$H[U_d(r, z)] = \bar{U}_d(\xi_i z) = \int_a^b U_d(r, z)rC_1(\xi_i r)dr \tag{25}$$

the inverse transform of finite Hankel transform (25) is

$$U_d(r, z) = \sum_{\xi_i} \frac{\bar{U}_{di}(\xi_i, z)}{F(\xi_i)} C_1(\xi_i r) \tag{26}$$

where  $F(\xi_i) = \int_a^b rC_1^2(\xi_i r)dr$  (27)

Using the above definition and applying the finite Hankel transform for  $r$  in the inhomogeneous dynamic Eq. (12), we have

$$-\xi_i^2 \bar{U}_{\theta d}(\xi_i, z, t) = \frac{1}{C_\tau^2} \left[ \frac{\partial^2 \bar{U}_{\theta s}(\xi_i, z, t)}{\partial t^2} + \frac{\partial^2 \bar{U}_{\theta d}(\xi_i, z, t)}{\partial t^2} \right] - \left[ \frac{\partial^2 \bar{U}_{\theta s}(\xi_i, z, t)}{\partial z^2} + \frac{\partial^2 \bar{U}_{\theta d}(\xi_i, z, t)}{\partial z^2} \right] \tag{28}$$

The Laplace transform for time  $t$  and its inverse can be, respectively, defined as

$$\begin{aligned} L[f(t)] &= f^*(p) = \int_0^{+\infty} f(t)e^{-pt} dt \\ L^{-1}[f^*(p)] &= f(t) = \int_{\sigma-i\infty}^{\sigma+i\infty} f^*(p)e^{pt} dp \end{aligned} \quad (29)$$

where,  $p = \sigma + i\omega$  is a complex variable.

Applying Laplace transform for  $t$  to Eq. (28) yields

$$\begin{aligned} -\xi_i^2 \bar{U}_{\theta d}^*(\xi_i, z, p) &= \frac{1}{C_\tau} \{p^2 [\bar{U}_{\theta s}^*(\xi_i, z, p) + \bar{U}_{\theta d}^*(\xi_i, z, p)] - p \bar{U}_{\theta 0}(\xi_i, z) - \bar{V}_{\theta 0}(\xi_i, z)\} - \\ &\quad \left[ \frac{\partial^2 \bar{U}_{\theta s}^*(\xi_i, z, p)}{\partial z^2} + \frac{\partial^2 \bar{U}_{\theta d}^*(\xi_i, z, p)}{\partial z^2} \right] \end{aligned} \quad (30)$$

In order to ensure both  $U_{\theta s}(r, z, t)$  and  $U_{\theta d}(r, z, t)$  meet the free end conditions, we suppose

$$U_{\theta s}(r, z, t) = \sum_{n=0}^{\infty} \tilde{U}_{\theta s}(r, n, t) \cos \frac{n\pi z}{L}, \quad U_{\theta d}(r, z, t) = \sum_{n=0}^{\infty} \tilde{U}_{\theta d}(r, n, t) \cos \frac{n\pi z}{L} \quad (31)$$

According to the following finite Fourier cosine transform and its inverse transform

$$\phi[f(z)] = F(n) = \int_0^L f(z) \cos \frac{n\pi z}{L} dz \quad n = 0, 1, 2, \dots \quad (32a)$$

$$\phi^{-1}[F(n)] = f(z) = \frac{1}{L} F(0) + \frac{2}{L} \sum_{n=1}^{\infty} F(n) \cos \frac{n\pi z}{L} \quad (32b)$$

$\tilde{U}_{\theta s}$  and  $\tilde{U}_{\theta d}$  can be represented as

$$\tilde{U}_{\theta s}(r, 0, t) = \frac{1}{L} \int_0^L U_{\theta s}(r, z, t) dz$$

$$\tilde{U}_{\theta s}(r, n, t) = \frac{2}{L} \int_0^L U_{\theta s}(r, z, t) \cos \frac{n\pi z}{L} dz \quad n = 1, 2, 3, \dots \quad (33a,b)$$

$$\tilde{U}_{\theta d}(r, 0, t) = \frac{1}{L} \int_0^L U_{\theta d}(r, z, t) dz \quad (33c)$$

$$\tilde{U}_{\theta d}(r, n, t) = \frac{2}{L} \int_0^L U_{\theta d}(r, z, t) \cos \frac{n\pi z}{L} dz \quad n = 1, 2, 3, \dots \quad (33d)$$

Applying Eq. (33) to Eq. (30) gives

$$\begin{aligned} -\xi_i^2 \tilde{U}_{\theta d}^*(\xi_i, n, p) &= \frac{1}{C_\tau} \{p^2 [\tilde{U}_{\theta s}^*(\xi_i, n, p) + \tilde{U}_{\theta d}^*(\xi_i, n, p)] - p \tilde{U}_{\theta 0}(\xi_i, n) - \tilde{V}_{\theta 0}(\xi_i, n)\} + \\ &\quad \frac{n^2 \pi^2}{L^2} [\tilde{U}_{\theta s}^*(\xi_i, n, p) + \tilde{U}_{\theta d}^*(\xi_i, n, p)], \quad (n = 0, 1, 2, 3, \dots) \end{aligned} \quad (34)$$

where,

$$\begin{aligned}
 \tilde{U}_{\theta d}^*(\xi_i, 0, p) &= \frac{1}{L} \int_0^L \bar{U}_{\theta d}^*(\xi_i, z, p) dz, & \tilde{U}_{\theta d}^*(\xi_i, n, p) &= \frac{2}{L} \int_0^L \bar{U}_{\theta d}^*(\xi_i, z, p) \cos \frac{n\pi z}{L} dz \\
 \tilde{U}_{\theta s}^*(\xi_i, 0, p) &= \frac{1}{L} \int_0^L \bar{U}_{\theta s}^*(\xi_i, z, p) dz, & \tilde{U}_{\theta s}^*(\xi_i, n, p) &= \frac{2}{L} \int_0^L \bar{U}_{\theta s}^*(\xi_i, z, p) \cos \frac{n\pi z}{L} dz \\
 \tilde{U}_{\theta 0}(\xi_i, 0) &= \frac{1}{L} \int_0^L \bar{U}_{\theta 0}(\xi_i, z) dz, & \tilde{U}_{\theta 0}(\xi_i, n) &= \frac{2}{L} \int_0^L \bar{U}_{\theta 0}(\xi_i, z) \cos \frac{n\pi z}{L} dz \\
 \tilde{V}_{\theta 0}(\xi_i, 0) &= \frac{1}{L} \int_0^L \bar{V}_{\theta 0}(\xi_i, z) dz, & \tilde{V}_{\theta 0}(\xi_i, n) &= \frac{2}{L} \int_0^L \bar{V}_{\theta 0}(\xi_i, z) \cos \frac{n\pi z}{L} dz
 \end{aligned} \tag{35a-h}$$

Eq. (34) can be simplified as

$$\tilde{U}_{\theta d}(\xi_i, n, p) = -\tilde{U}_{\theta s}^*(\xi_i, n, p) + \frac{\omega_i^2}{p^2 + x^2} \tilde{U}_{\theta s}^*(\xi_i, n, p) - \frac{p}{p^2 + x^2} \tilde{U}_{\theta 0}(\xi_i, n) - \frac{1}{p^2 + x^2} \tilde{V}_{\theta 0}(\xi_i, n) \tag{36}$$

where,

$$\omega_i = \xi_i C_\tau, \quad \chi = \sqrt{\omega_i^2 + \frac{n^2 \pi^2 C_\tau^2}{L^2}} \tag{37}$$

Applying the inverse Laplace transform to Eq. (36) yields

$$\begin{aligned}
 \tilde{U}_{\theta d}(\xi_i, n, t) &= -\tilde{U}_{\theta s}(\xi_i, n, t) + \frac{\omega_i^2}{x^2} \sin x t * \tilde{U}_{\theta s}(\xi_i, n, p) - \tilde{U}_{\theta 0}(\xi_i, n) \cos x t - \frac{\sin x}{x} \tilde{V}_{\theta 0}(\xi_i, n) \\
 &(n = 0, 1, 2, 3, \dots)
 \end{aligned} \tag{38}$$

where

$$\sin x t * \tilde{U}_{\theta s}(\xi_i, n, p) = \int_0^t \sin x(t - \tau) \tilde{U}_{\theta s}(\xi_i, n, \tau) d\tau \tag{39}$$

The inverse Fourier transform of Eq. (38) gives

$$\bar{U}_{\theta d}(\xi_i, z, t) = \sum_{n=0}^{\infty} \tilde{U}_{\theta d}(\xi_i, n, t) \cos \frac{n\pi z}{L} \tag{40}$$

The inverse Hankel transform of Eq. (40) gives

$$U_{\theta d}(r, z, t) = \sum_{\xi_i} \frac{\sum_{n=0}^{\infty} \tilde{U}_{\theta d}(\xi_i, n, t) \cos \frac{n\pi z}{L}}{F(\xi_i)} C_1(\xi_i r) \tag{41}$$

From Eqs. (8), (11) and (41), the analytical expression of the elastodynamic solution is represented as

$$U_{\theta}(r, z, t) = \frac{a^2}{2G} \left( \frac{r}{b^2} - \frac{1}{r} \right) \sum_{n=0}^{\infty} \tilde{A}(n, t) \cos \frac{n\pi z}{L} + \sum_{\xi_i} \frac{\sum_{n=0}^{\infty} \tilde{U}_{\theta d}(\xi_i, n, t) \cos \frac{n\pi z}{L}}{F(\xi_i)} C_1(\xi_i r) \tag{42}$$

where 
$$\tilde{A}(0, t) = \frac{1}{L} \int_0^L A(z, t) dz$$

$$\tilde{A}(n, t) = \frac{2}{L} \int_0^L A(z, t) \cos \frac{n\pi z}{L} dz \quad (n = 1, 2, 3, \dots) \tag{43}$$

From Eqs. (1) and (2), the analytical expression of the dynamic shear stress can be written as

$$\begin{aligned} \tau_{r\theta}(r, z, t) &= \frac{a^2}{r^2} \sum_{n=0}^{\infty} \tilde{A}(n, t) \cos \frac{n\pi z}{L} + G \sum_{\xi_i} \frac{\sum_{n=0}^{\infty} \tilde{U}_{\theta d}(\xi_i, n, t) \cos \frac{n\pi z}{L}}{F(\xi_i)} \left[ \frac{d}{dr} C_1(\xi_i r) - \frac{C_1(\xi_i r)}{r} \right] \\ \tau_{\theta z}(r, z, t) &= \frac{a^2}{2} \left( \frac{r}{b^2} - \frac{1}{r} \right) \sum_{n=0}^{\infty} \left( -\frac{n\pi}{L} \right) \tilde{A}(n, t) \sin \frac{n\pi z}{L} - G \frac{n\pi}{L} \sum_{\xi_i} \frac{\sum_{n=0}^{\infty} \tilde{U}_{\theta d}(\xi_i, n, t) \sin \frac{n\pi z}{L}}{F(\xi_i)} C_1(\xi_i r) \end{aligned} \tag{44}$$

### 3. Example and discussion

In practical engineering, torsional impact load with exponential decay is more common, which can be represented as

$$A(z, t) = \begin{cases} 0 & t < 0 \\ \tau_0 z e^{-\alpha t} & t \geq 0 \end{cases} \tag{45}$$

The initial condition before the loading is considered as

$$U_{\theta}(r, z, 0) = U_{\theta 0}(r, z) = 0, \quad \frac{\partial U_{\theta}(r, z, 0)}{\partial t} = V_{\theta 0}(r, z) = 0 \tag{46}$$

From Eqs. (45), (46) and (42), the response of the tangent displacement is given by

$$\begin{aligned} U_{\theta}(r, z, t) &= \frac{\tau_0 a^2}{2G} \left( \frac{r}{b^2} - \frac{1}{r} \right) e^{-\alpha t} \left\{ \frac{L}{2} + \frac{2}{\pi^2} \sum_{n=1}^{\infty} n^2 [(-1)^n - 1] \cos \frac{n\pi z}{L} \right\} + \\ &\sum_{\xi_i} \frac{1}{F(\xi_i)} \left\{ \frac{\tau_0 L J_1(\xi_i b)}{G \pi \xi_i^2 J_a} \frac{[-\alpha C_{\tau} \xi_i \sin(\omega_i t) + \omega_i^2 \cos \omega_i t + \alpha^2 e^{-\alpha t}]}{\alpha^2 + \omega_i^2} + \right. \\ &\left. \frac{4 \tau_0 L J_1(\xi_i b)}{\pi^3 J_a} \sum_{n=1}^{\infty} \frac{1}{n^2} [(-1)^n - 1] \left[ \frac{e^{-\alpha t}}{G \xi_i^2} - \frac{1}{\rho x} \right] \cos \frac{n\pi z}{L} \right\} C_1(\xi_i r) \end{aligned} \tag{47}$$

Substituting Eq. (47) into Eq. (44), the expressions of dynamic shear stress are written as

$$\begin{aligned} \tau_{r\theta}(r, z, t) = & \frac{\tau_0 a^2}{r^2} e^{-\alpha t} \left\{ \frac{L}{2} + \frac{2}{\pi^2} \sum_{n=0}^{\infty} n^2 [(-1)^n - 1] \cos \frac{n\pi z}{L} \right\} + \\ & \sum_{\xi_i} \frac{1}{F(\xi_i)} \left\{ \frac{\tau_0 L J_1(\xi_i b)}{G \pi \xi_i^2 J_a} \frac{[-\alpha \omega_i \sin \omega_i t + \omega_i^2 \cos \omega_i t + \alpha^2 e^{-\alpha t}]}{\alpha^2 + \omega_i^2} + \right. \\ & \left. \frac{4 \tau_0 L J_1(\xi_i b)}{\pi^3 J_a} \sum_{n=1}^{\infty} \frac{1}{n^2} [(-1)^n - 1] \left[ \frac{e^{-\alpha t}}{G \xi_i^2} - \frac{1}{\rho \chi} \frac{\alpha \sin \chi t - \chi \cos \chi t + \chi e^{-\alpha t}}{\alpha^2 + \chi^2} \right] \cos \frac{n\pi z}{L} \right\} \\ & \times \left[ \xi_i C_0(\xi_i r) - \frac{2}{r} C_1(\xi_i r) \right] \end{aligned} \quad (48)$$

$$\begin{aligned} \tau_{\theta z}(r, z, t) = & \frac{\tau_0 a^2}{2} \left( \frac{r}{b^2} - \frac{1}{r} \right) e^{-\alpha t} \sum_{n=1}^{\infty} \frac{1}{n\pi} [1 + (-1)^{n+1}] \sin \frac{n\pi z}{L} - \sum_{\xi_i} \frac{1}{F(\xi_i)} \frac{4G \tau_0 J_1(\xi_i b)}{\pi^2 J_a} C_1(\xi_i r) \times \\ & \left\{ \sum_{n=1}^{\infty} \frac{1}{n} [(-1)^n - 1] \left( \frac{e^{-\alpha t}}{G \xi_i^2} - \frac{1}{\rho \chi} \frac{\alpha \sin \chi t - \chi \cos \chi t + \chi e^{-\alpha t}}{\alpha^2 + \chi^2} \right) \sin \frac{n\pi z}{L} \right\} \end{aligned} \quad (49)$$

where  $C_0(\xi_i r) = J_0(\xi_i r) Y_0(\xi_i b) - J_0(\xi_i b) Y_0(\xi_i r)$  (50)

and  $J_0(\xi r)$  and  $Y_0(\xi r)$  are, respectively, zero order Bessel function of the first and the second kinds.

In example calculations, to improve the convergence of these series in the expression of the solution, we consult a particularly useful book given in Lighthill (1958). Material properties of the structure are considered as:  $G = 80$  Gpa,  $\rho = 7800$  kg/m<sup>3</sup>. The thickness of hollow cylinders are, respectively,  $(b - a)/a = 20$  and  $(b - a)/a = 2$ , where  $a = 0.01$  m. In order to make the problem easy to deal with, the all variables are taken as the form of dimensionless:  $T^* = tC_\tau/a$ ,  $R^* = (r-a)/(b-a)$ ,  $Z^* = z/L$ ,  $\tau_{r\theta}^* = \tau_{r\theta}/\tau_0$ ,  $\tau_{\theta z}^* = \tau_{\theta z}/\tau_0$ ,  $U_\theta^* = U_\theta/\tau_0$  (m/pa).

Fig. 2 to Fig. 7 show that the curves of shear stress and tangent displacement vary with  $z^*$  and time  $T^*$  when the finitely long, hollow cylinder with  $(b - a)/a = 20$  is subjected to torsional impact, during  $T^* \leq 20$ . For this structure and the corresponding parameters, the reflecting effects of the shear stress wave in the structure are excluded. From Fig. 2 and Fig. 3, it can be seen that shear stress  $\tau_{r\theta}^*$  and  $\tau_{\theta z}^*$  meet the corresponding boundary condition at both the internal boundary, and two ends of the finitely long hollow cylinder. From Fig. 5 to Fig. 7, it can be seen that there is abrupt leap at the wavefront of the shear stress wave and tangent displacement when  $T^* = 1$ . When the stress wave reaches the place  $R^* = 1$ , and as the wavefront spreading far from the place  $R^* = 1$  to the external boundary during  $T^* > 1$ , the responses of the shear stress wave and tangent displacement at this point will gradually tend to the quasi-static solution of the point. In order to describe the wave effect of the shear stress and tangent displacement in the finitely long hollow cylinder subjected to the torsional impact load, much clearly, Fig. 8 and Fig. 9 show the responding histories of the shear stress and the tangent displacement at the place  $Z^* = 0.5$  (the middle part of the finitely long, hollow cylinder). For a certain point in the hollow cylinder where the stress wave

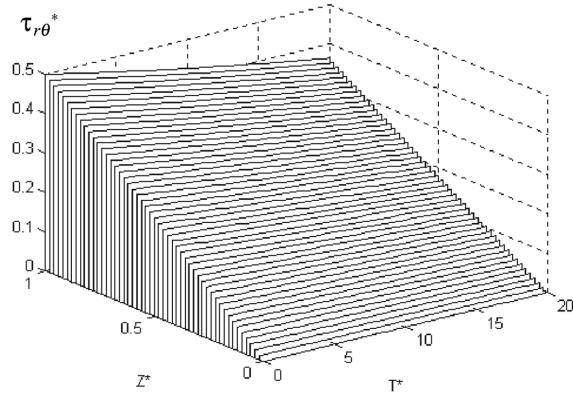


Fig. 2 The responding histories of shear stress  $\tau_{r\theta}^*$  in finitely long hollow cylinder under torsion shock.  $R^* = 0$ ,  $(b - a)/a = 20$ ,  $Z^* = z/L$ ,  $R^* = (r - a)/(b - a)$ ,  $T^* = tC_L/a$ ,  $\tau_{r\theta}^* = \tau_{r\theta}/\tau_0$

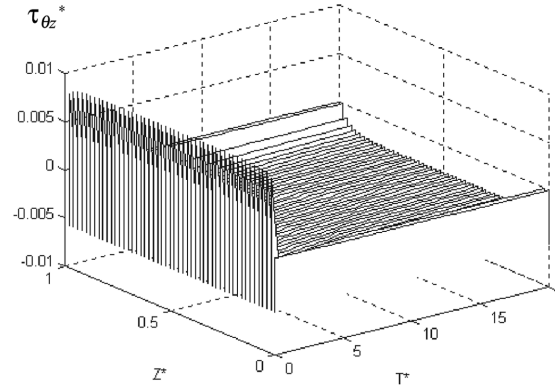


Fig. 3 The responding histories of shear stress  $\tau_{\theta z}^*$  in finitely long hollow cylinder under torsion shock.  $R^* = 0$ ,  $(b - a)/a = 20$ ,  $Z^* = z/L$ ,  $R^* = (r - a)/(b - a)$ ,  $T^* = tC_L/a$ ,  $\tau_{\theta z}^* = \tau_{\theta z}/\tau_0$

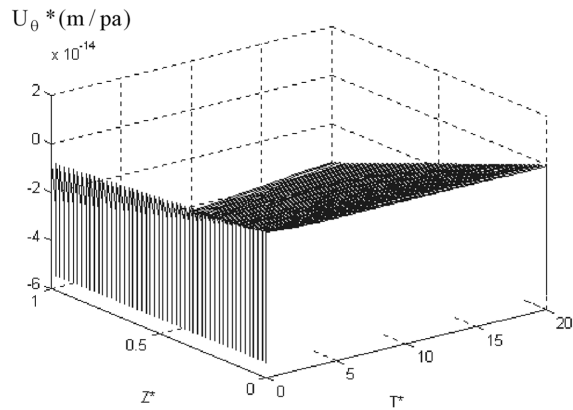


Fig. 4 The responding histories of tangent displacement  $U_{\theta}^*$  in finitely long hollow cylinder under torsion shock.  $R^* = 0$ ,  $(b - a)/a = 20$ ,  $R^* = (r - a)/(b - a)$ ,  $T^* = tC_L/a$ ,  $Z^* = z/L$ ,  $U_{\theta}^* = U_{\theta}/\tau_0$

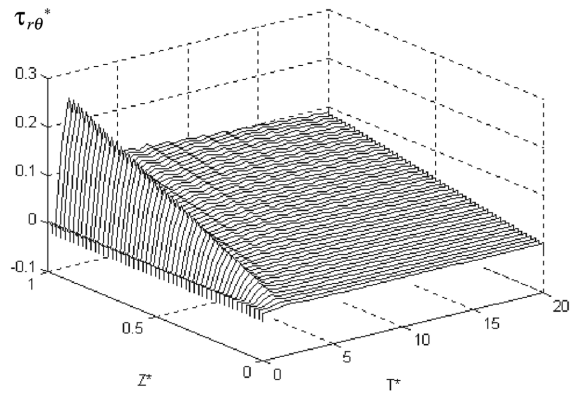


Fig. 5 The responding histories of shear stress  $\tau_{r\theta}^*$  in finitely long hollow cylinder under torsion shock.  $R^* = 1$ ,  $(b - a)/a = 20$ ,  $Z^* = z/L$ ,  $R^* = (r - a)/(b - a)$ ,  $T^* = tC_L/a$ ,  $\tau_{r\theta}^* = \tau_{r\theta}/\tau_0$

has not reached, the response value of the stress wave equals to zero. When the wavefront arrives at the point, the response value is the biggest. When wavefront goes away from the point, the corresponding response value tends to the quasi-static solution of the point.

For the finitely long hollow cylinder with  $(b - a)/a = 2$  subjected to the torsional impact, the shear stress varying with the axial variable  $z$  and time  $t$  are, respectively, shown in Fig. 10 to Fig. 15, for  $0 \leq T^* \leq 20$ . During  $T^* > 1$ , any point in this structure will be influenced by reflected wave between the inner and outer wall. Because of the influence of the incessant reflection of the wave, the responses at any point in the structure will oscillate strongly.

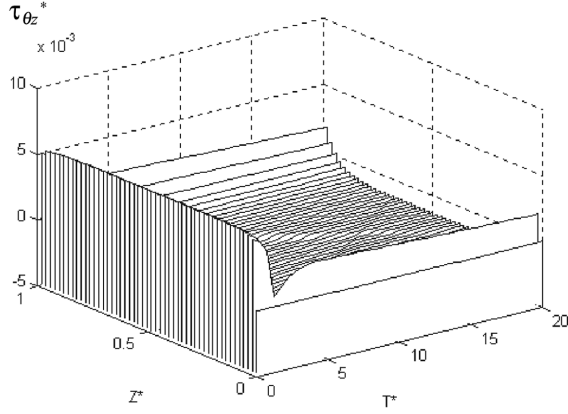


Fig. 6 The responding histories of shear stress  $\tau_{z\theta}^*$  in finitely long hollow cylinder under torsion shock.  $R^* = 1$ ,  $(b - a)/a = 20$ ,  $Z^* = z/L$ ,  $T^* = tC_L/a$ ,  $R^* = (r - a)/(b - a)$ ,  $\tau_{zr\theta}^* = \tau_{z\theta}/\tau_0$

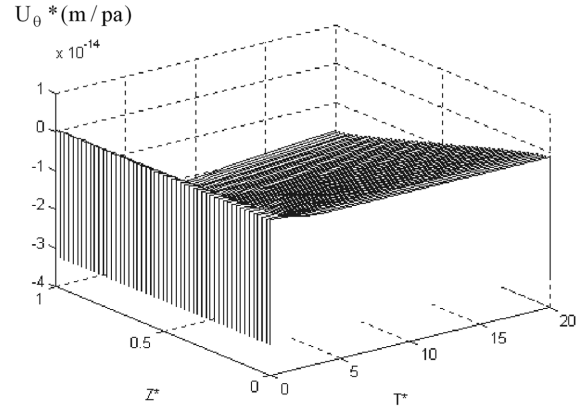


Fig. 7 The responding histories of tangent displacement  $U_\theta^*$  in finitely long hollow cylinder under torsion shock.  $R^* = 1$ ,  $(b - a)/a = 20$ ,  $T^* = tC_L/a$ ,  $R^* = (r - a)/(b - a)$ ,  $Z^* = z/L$ ,  $U_\theta^* = U_\theta/\tau_0$

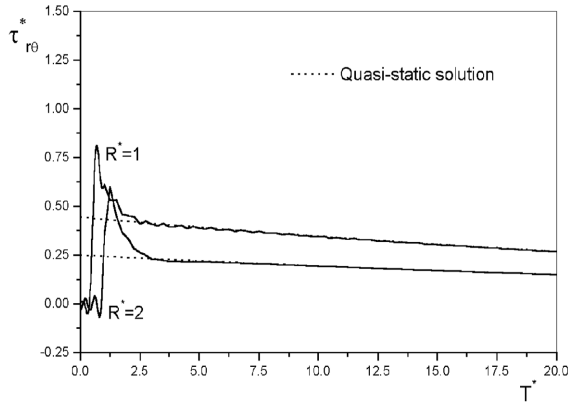


Fig. 8 The responding histories of shear stress  $\tau_{r\theta}^*$  in finitely long hollow cylinder under torsion shock.  $(b - a)/a = 20$ ,  $Z^* = z/L = 0.5$ ,  $R^* = (r - a)/(b - a)$ ,  $T^* = tC_L/a$ ,  $\tau_{r\theta}^* = \tau_{r\theta}/\tau_0$

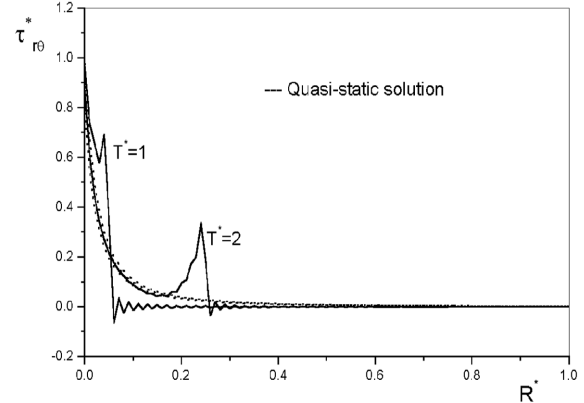


Fig. 9 The distributions of shear stress  $\tau_{r\theta}^*$  in finitely long hollow cylinder under torsion shock.  $(b - a)/a = 20$ ,  $Z^* = z/L = 0.5$ ,  $R^* = (r - a)/(b - a)$ ,  $T^* = tC_L/a$ ,  $\tau_{r\theta}^* = \tau_{r\theta}/\tau_0$

In order to prove the validity of the analytical method and the solving process further, a dynamic finite element solution for the same example used in the solution is also achieved by using ABAQUS finite element analytical card. In this dynamic equation of elastic system, using the Halmiton principle, the dynamic equation of the finite element is written as

$$[K]\{d\} + [M]\{\ddot{d}\} = \{F(t)\} \quad (51)$$

where  $[K]$  is the stiff matrix,  $[M]$  is the weight matrix,  $\{d\}$  is the displacement of the knot points

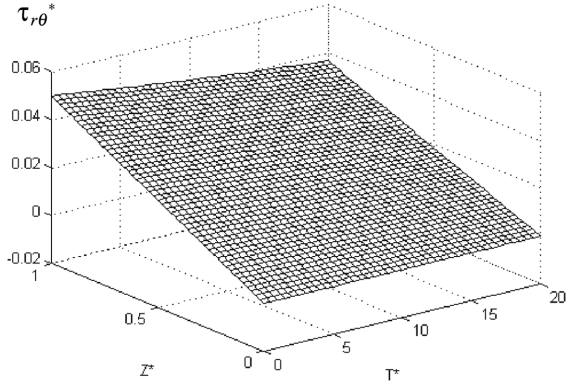


Fig. 10 The responding histories of shear stress  $\tau_{r\theta}^*$  in finitely long hollow cylinder under torsion shock.  $R^* = 0$ ,  $(b - a)/a = 2$ ,  $Z^* = z/L$ ,  $T^* = tC_L/a$ ,  $R^* = (r - a)/(b - a)$ ,  $\tau_{r\theta}^* = \tau_{r\theta}/\tau_0$

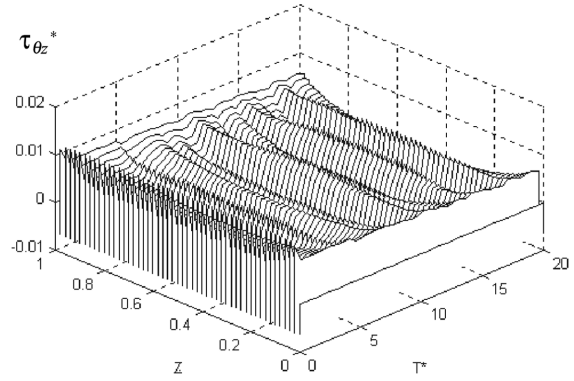


Fig. 11 The responding histories of shear stress  $\tau_{z\theta}^*$  in finitely long hollow cylinder under torsion shock.  $R^* = 0$ ,  $(b - a)/a = 2$ ,  $Z^* = z/L$ ,  $T^* = tC_L/a$ ,  $R^* = (r - a)/(b - a)$ ,  $\tau_{z\theta}^* = \tau_{z\theta}/\tau_0$

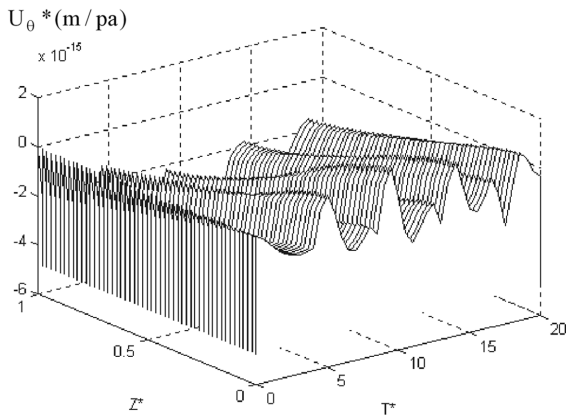


Fig. 12 The responding histories of tangent displacement  $U_\theta^*$  in finitely long hollow cylinder under torsion shock.  $R^* = 1$ ,  $(b - a)/a = 2$ ,  $Z^* = z/L$ ,  $R^* = (r - a)/(b - a)$ ,  $T^* = tC_L/a$ ,  $U_\theta^* = U_\theta/\tau_0$

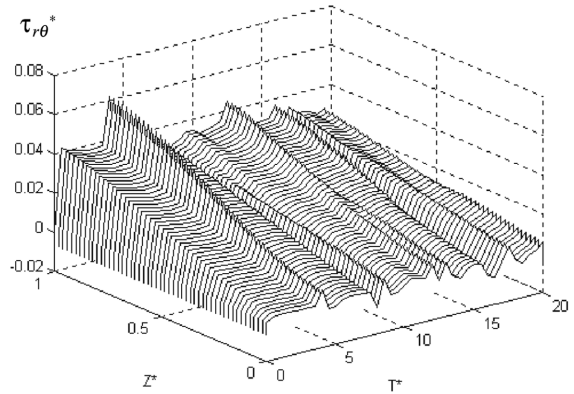


Fig. 13 The responding histories of shear stress  $\tau_{r\theta}^*$  in finitely long hollow cylinder under torsion shock.  $R^* = 0.1$ ,  $(b - a)/a = 2$ ,  $Z^* = z/L$ ,  $R^* = (r - a)/(b - a)$ ,  $T^* = tC_L/a$ ,  $\tau_{r\theta}^* = \tau_{r\theta}/\tau_0$

and  $\{F(t)\}$  is the dynamic load. In the solving process of the dynamic finite element, using a directly integral method, the solution of the dynamic Eq. (51) can be obtained by ABAQUS program card. Considering Fig. 1, the finite element model and net for the middle plane at  $z^* = 0.5$  of the finitely long hollow cylinder can be shown in Fig. 16. The geometry size and material property are the same as those in the theoretical solution and time step is taken as  $\Delta t = 0.01a/C_L$ . The relative error is less than 1%.

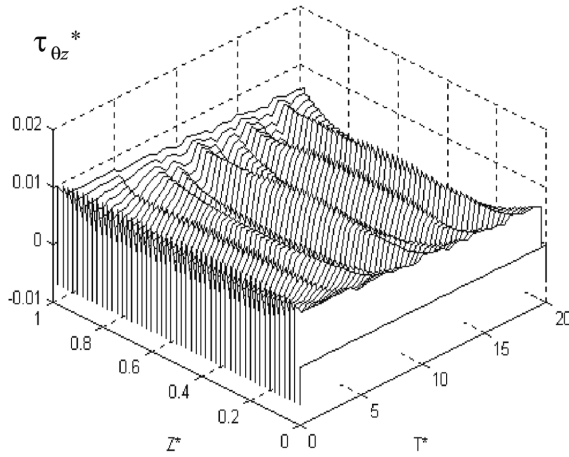


Fig. 14 The responding histories of shear stress  $\tau_{z\theta}^*$  in finitely long hollow cylinder under torsion shock.  $R^* = 0.1$ ,  $(b - a)/a = 2$ ,  $Z^* = z/L$ ,  $T^* = tC_L/a$ ,  $R^* = (r - a)/(b - a)$ ,  $\tau_{z\theta}^* = \tau_{z\theta}/\tau_0$

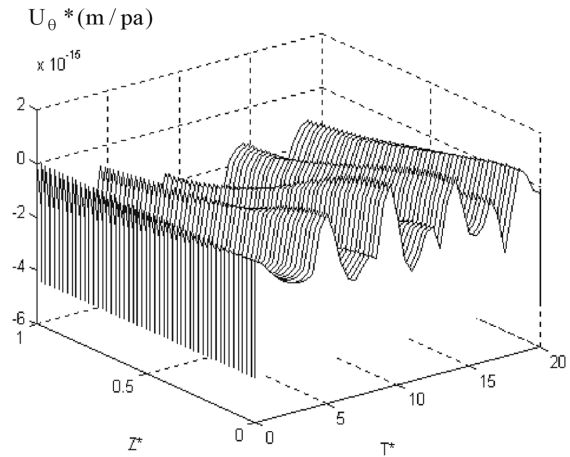


Fig. 15 The responding histories of tangent displacement  $U_{\theta}^*$  in finitely long hollow cylinder under torsion shock.  $R^* = 0.1$ ,  $(b - a)/a = 2$ ,  $T^* = tC_L/a$ ,  $R^* = (r - a)/(b - a)$ ,  $Z^* = z/L$ ,  $U_{\theta}^* = U_{\theta}/\tau_0$

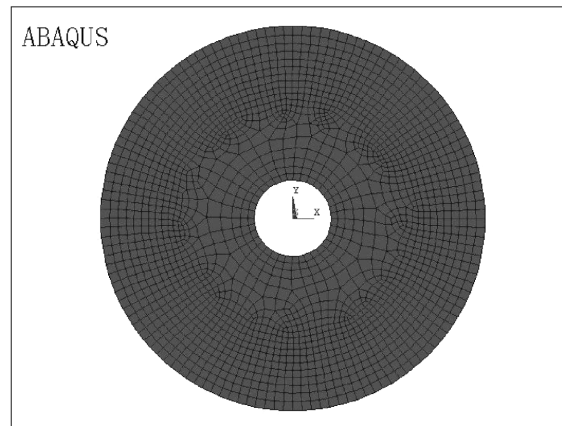


Fig. 16 The finite element net for the middle plane at  $z^* = 0.5$  in finite length of hollow cylinder under sudden torsion load for  $\beta = 0$ ,  $(b - a)/a = 5$

#### 4. Conclusions

It is noted that while solving the present problem, the number of eigenvalue terms was taken as 40, and the relative error in the results obtained was less than 1%. The features of the stress waves propagating in the finitely long, hollow cylinder along the radial direction are clearly shown in Figs. 2-9. The responses of shear stress at which the wavefront of stress wave has not arrived equal to zero. The responses of shear stress at which the wavefront arrives appear in the maximum value and strong discontinuous effects. The propagation of the wavefront decays and the dynamic stress approaches to the quasi-static stress at the same point when time is large and the effect of reflected wave does not appear.

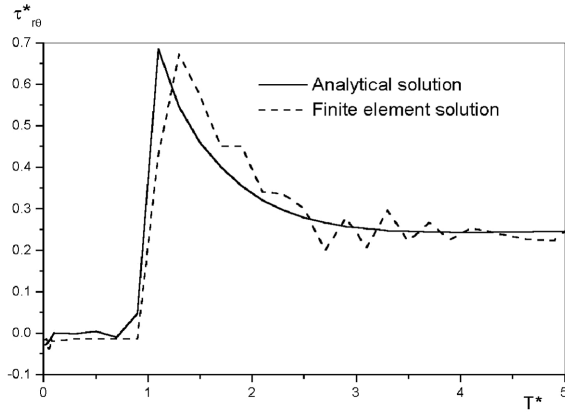


Fig. 17 The response histories of shear stress in the  $r$ - $\theta$  plane at  $z^* = 0.5$  in finite length hollow cylinder under sudden torsion load for  $\beta = 0$ ,  $(b - a)/a = 5$ ,  $R^* = (r - a)/a$ ,  $T^* = tC_L/a$ ,  $\tau_{r\theta}^* = \tau_{r\theta}/\tau_0$

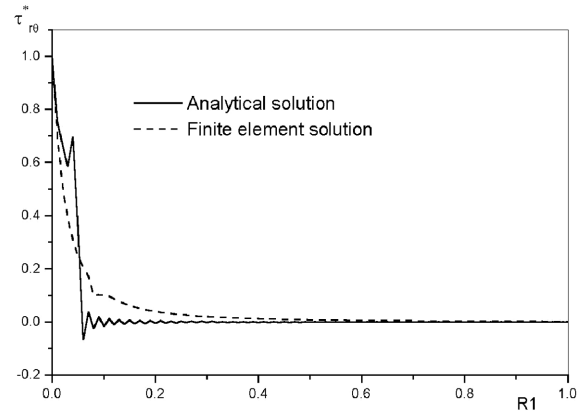


Fig. 18 The distribution of shear stress in the  $r$ - $\theta$  plane at  $z^* = 0.5$  in finite length hollow cylinder under sudden torsion load for  $\beta = 0$ ,  $(b - a)/a = 5$ ,  $R1 = (r - a)/(b - a)$ ,  $T^* = tC_L/(b - a)$ ,  $T^* = 0.1$ ,  $\tau_{r\theta}^* = \tau_{r\theta}/\tau_0$

Comparing the theoretical solution with the finite element solution shown in Fig. 17 and Fig. 18, it can be found that two kinds of results obtained by making use of two different solving methods are suitably approached. Therefore, it is further concluded that the method and computing process of the theoretical solution are effective and accurate.

It is noted that the key to solve the problem of stress wave propagation using a dynamic finite element method is how to select calculating time step corresponding the finite element mesh. Therefore, it is very difficult to exactly obtain the maximum amplitude of stress wavefront by using the dynamic finite element calculation. An analytical solution can give an exact expression of stress wave propagation, which can be used to directly discuss some physical characters of stress wave propagation.

From this knowledge of the response histories for the elastodynamic solution to finitely long hollow cylinder subjected to torsional impact load presented in this paper, it can be assessed that the dynamic intensity of the structure subjected to torsional impact load in various special engineering requirements such as mechanical drilling, petroleum drilling and automatic fasten of steel structure's fastening bolts, and can also use it as a reference of various approximate theories.

## Acknowledgements

The authors thank the referees for their valuable comments.

## References

- Armenaakas, A.E. (1965), "Torsional waves in composite rods", *J. Acoustical Soc. Am.*, **38**, 439-446.  
 Carcione, J.M. and Seriani, G. (1998), "Torsional waves in lossy cylinders", *J. Acoustical Soc. Am.*, **103**, 760-765.

- Carcione, J.M. and Flavio, P. (2000), "Simulation of stress waves in attenuating drill strings including piezoelectric sources and sensors", *J. Acoustical Soc. Am.*, **108**, 53-64.
- Cho, H., Kardomateas, G.A. and Valle, C.S. (1998), "Elastodynamic solution for the thermal shock stress in an orthotropic thick cylinder shell", *J. Appl. Mech.*, ASME, **65**(1), 184-193.
- Cinelli, G. (1965), "An extension of the finite Hankel transform and application", *Int. J. Engng. Sci.*, **3**, 539-550.
- Cinelli, G. (1966), "Dynamic vibrations and stress in the elastic cylinders and spheres", *J. Appl. Mech.*, ASME, 825-830.
- Clark, S.K. (1956), "Torsional wave propagation in hollow cylindrical bars", *J. Acoustical Soc. Am.*, **28**, 1163-1165.
- Eringen, A.C. and Suhubi, E.S. (1975), *Elastodynamics*, Vol. 2, (Linear Theory) Academic Press. New York.
- Gazis, D.C. (1959a), "Three-dimensional investigation of the propagation of waves in hollow circular cylinders, I. Analytic foundation", *J. Acoustical Soc. Am.*, **31**, 568-573.
- Gazis, D.C. (1959b), "Three-dimensional investigation of the propagation of waves in hollow circular cylinders, II. Analytic foundation", *J. Acoustical Soc. Am.*, **31**, 573-578.
- Haines, D.W. and Lee, P.C.Y. (1971), "Approximate theory of torsional wave propagation in elastic circular composite cylinders", *J. Acoustical Soc. Am.*, **49**, 211-219.
- Kim, J.O. and Haim, H.H. (1991), "Torsional stress waves in a circular cylinder with a modulated surface", *J. Appl. Mech.*, ASME, **58**, 710-715.
- Lighthill, M.J. (1958), *An Introduction to Fourier Analysis and Generalized Function*, Cambridge University Press.
- Liu, C.G. and Wang, D. (1995), "Spread problem on torsion wave in a infinite long elastic hollow cylinder", <Advance progress on dynamic mechanics> Science Publisher in China.
- Pao, Y.H. and Ceranoglu, A.N. (1978), "Determination of transient responses of a thick-walled spherical shell by the ray theory", *J. Appl. Mech.*, ASME, **45**, 114-122.
- Soldatos, K.P. and Ye, J.Q. (1994), "Wave propagation in anisotropic laminated hollow cylinders of infinite extent", *J. Acoustics Soc. Am.*, **96**(5), 744-752.
- Wang, X., Zhang, K. and Zhang, W. (2000), "Theoretical solution and finite element solution for an orthotropic thick cylindrical shell under impact load", *J. Sound Vib.*, **236**, 129-140.

## Notation

$U_\theta(r, z, t), U_r, U_z$	: tangential, radial and axial displacements
$\gamma_{ij}$ and $\tau_{ij}$	: shear strains and shear stresses
$\tau_{r\theta}$	: shear stress in the $r\theta$ plane
$\tau_{\theta z}$	: shear stress in the $\theta z$ plane
$U_{\theta s}$	: quasi-static displacement solution
$U_{\theta d}$	: displacement solution of nonhomogeneous dynamic equation
$G$	: shear modulus
$\rho$ and $t$	: density of the material and time variable
$a, b$ and $L$	: internal radii, external radii and length of hollow cylinder
$C_\tau = \sqrt{G/\rho}$	: elastic wave speed
$A(z, t)$	: torsion impact load function
$J_1(\xi_i r)$ and $Y_1(\xi_i r)$	: first order Bessel function of the first and second kinds
$J_0(\xi_i r)$ and $Y_0(\xi_i r)$	: zero <sup>th</sup> order Bessel function of the first and second kinds
$\xi_i (i=1, 2, 3, \dots)$	: positive eigenroots

## Nondimensional Quantities

$$T^* = tC_\tau/a, \quad R^* = (r-a)/a, \quad R1 = (r-a)/(b-a), \quad Z^* = z/L, \quad \tau_{r\theta}^* = \tau_{r\theta}/\tau_0$$

$$\tau_{\theta z}^* = \tau_{\theta z}/\tau_0, \quad U_\theta^* = U_\theta/\tau_0 \quad (m/Pa)$$